Journal of Alloys and Compounds 513 (2012) 112–117

Contents lists available at SciVerse ScienceDirect

Journal of Alloys and Compounds

journal homepage: www.elsevier.com/locate/jallcom

Flow behaviors and processing maps of as-cast and as-homogenized AZ91 alloy

Meng Mu [a,*], Zhang Zhi-min [b], Zhang Bao-hong [b], Dou Jin [b]

[a] School of Mechanical Engineering & Automation, North University of China, Taiyuan 030051, China
[b] College of Materials Science and Engineering, North University of China, Taiyuan 030051, China

ARTICLE INFO

Article history:
Received 22 July 2011
Accepted 28 September 2011
Available online 17 October 2011

Keywords:
AZ91 alloy
Flow behavior
Processing map

ABSTRACT

Compression tests of as-cast and as-homogenized AZ91 alloy were performed at the temperature range from 473 K to 673 K and the strain rate range from 0.001 s^{-1} to 5 s^{-1}, and the flow stress data obtained from the tests were used to develop the processing maps. By analysis, the main differences are as follows: the flow stress of the as-cast AZ91 alloy is higher at the lower temperatures (473 K) because of the strengthening β-phase distributing along grain boundaries. The efficiency of power dissipation of as-homogenized AZ91 alloy is greater than the as-cast state below 650 K because of a larger proportion of twining and/or DRX, and the as-homogenized state still owes the characteristics of stable flow at 473 K/0.001 s^{-1}. The optimum deformation parameters gained by the processing maps and microstructure are the same for different states, and the temperature and strain rate, respectively, are range from 623 K to 673 K and from 0.001 s^{-1} to 0.03 s^{-1}.

1. Introduction

The combination of low density and moderate strength makes magnesium alloys well suited for applications where weight is of critical importance. Several attempts have been made to search for optimum deformation conditions for magnesium alloys [1–5], since the unfavorable deformation behavior of magnesium at ambient temperature causes difficulties as a result of its hexagonal close packed crystal structure. They have studied the micro-structural development in AZ91 alloy during hot working and have characterized the micro-structural features with reference to the associated mechanisms such as twinning, dynamic recovery (DRV) and dynamic recrystallization (DRX) under limited deformation conditions. However, almost no attention has been paid to the condition of ingot before deformation. AZ91 cast ingot usually contains large amounts of $Mg_{17}Al_{12}$ divorced eutectics distributing along the grain boundary, however before hot deformation, these compounds are usually artificially dissolved into matrix after a routine homogenization treatment. Hence, possible influence of different initial ingot before deformation on the evolution of deformation microstructure has not been well investigated yet.

Processing map on the basis of dynamic material model (DMM), established by Prasad and co-workers recently [6,7,3], has been widely used to understand the hot workability of many materials, especially for some materials which are difficult to deform owing to low stacking fault energy on the basal planes [8] and wide extended dislocation, the dislocation formed in the magnesium alloy is hard to cross slip and climb. DMM considers the complementary relationship between the rate of visco-plastic heat generation induced by deformation and the rate of energy dissipation associated with micro-structural mechanisms occurring during deformation. A non-dimensional efficiency index η is used to represent the power dissipation through micro-structural mechanisms and is given as [9]

$$\eta = \frac{2m}{m-1}$$

where m is the strain rate sensitivity of the material, which is given as [10]

$$\left[\frac{\partial(\ln\sigma)}{\partial(\ln\dot{\varepsilon})}\right]_{\varepsilon,T} = m$$

The contour plot of the iso-efficiency η values on the temperature–strain rate field constitutes the processing map. With the change of deformation temperature and strain rate, η varies, which represents the characteristics of power dissipation through microstructure transition.

The instability map is developed on the basis of the extremum principles of irreversible thermodynamics applied for large plastic flow body [11]. The instability criterion is given as

$$\xi(\dot{\varepsilon}) = \frac{\partial \ln(m/(m-1))}{\partial \ln \dot{\varepsilon}} + m < 0$$

The variation of the instability parameter $\xi(\dot{\varepsilon})$ with the change of temperature and strain rate is applied to delineate the

* Corresponding author.
E-mail address: meng19831021@163.com (M. Mu).

0925-8388/$ – see front matter © 2011 Elsevier B.V. All rights reserved.
doi:10.1016/j.jallcom.2011.09.102

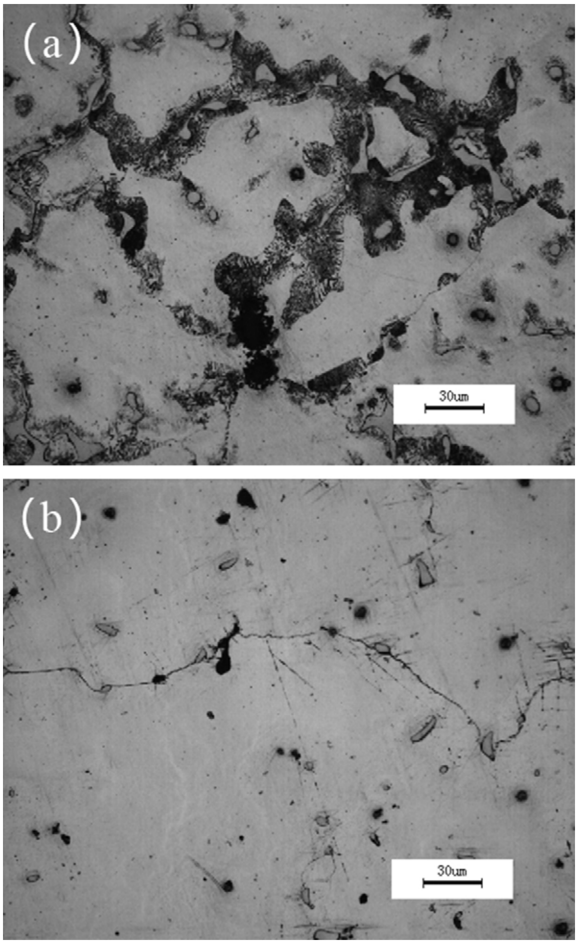

Fig. 1. The initial microstructure of the (a) as-cast AZ91 alloy and (b) as-homogenized AZ91 alloy.

temperature–strain rate regimes of flow instability on the processing map. A detailed description of the development of the model as well as the significance of η value in the interpretation of the domains has been given by Prasad et al. [12,11].

The present investigation is to study the hot deformation behaviors of as-cast and as-homogenized AZ91 alloy using hot compression test and the processing map technique. The aim is to clarify the effect of as-cast and as-homogenized initial ingot on the plastic flow behaviors and to determine optimum parameters for the forming processing.

2. Experimental

The composition (wt.%) of the as-cast AZ91 used in the test is as follows: Al, 9.1; Zn, 0.53; Mn, 0.20; Cu, <0.025; Fe, <0.004; Ni, <0.001; Si, <0.05; impurity, 0.01 and balance Mg. The initial microstructure of the as-cast AZ91 is given in Fig. 1(a). The as-cast AZ91 was homogenized at 673 K for 12 h, then water-quenched. The microstructure of the as-homogenized AZ91 is given in Fig. 1(b). The specimens were cut with dimension of Ø 8 mm × 12 mm. The specimens were compression deformed at the temperature range from 473 K to 673 K and the strain rate range from 0.001 s^{-1} to 5 s^{-1} on the Gleeble-1500 thermo-mechanical simulator. In order to reduce the deformed friction, a graphite lubricant was used between the specimens and the crossheads. The specimens were induction-heated to deformation temperatures at a heating rate of 3 K/s and held for 5 min in order to obtain a stable and uniformity temperature prior to deformation. After test, it was water-quenched to room temperature (RT).

The microstructures of the as-cast and as-homogenized AZ91 alloy after hot compression were studied by optical microscope (OM). The observation samples were cut out from the middle part of the deformed specimens with the observed faces perpendicular to the compression direction. After being polished to mirror state, the surface was etched by an acetic glycol solution (20 ml acetic acid, 1 ml HNO_3, 60 ml ethylene glycol and 19 ml distilled water).

The as-cast AZ91 alloy consists of a-Mg matrix surrounded by the eutectic consisting of (a + β) lamellar precipitates and massive β-$Mg_{17}Al_{12}$ intermetallic phases in Fig. 1(a). The massive phase contains, in addition to Mg and Al, small amount of Zn in it [13,14]. After homogenization, the AZ91 alloy has a microstructure of few small $Mg_{17}Al_{12}$ (β phase) particles on grain boundaries. Compared to the microstructure of as-cast AZ91 alloy, most $Mg_{17}Al_{12}$ particles have been dissolved into the a-Mg matrix, and the remained particles become very small.

3. Results and discussion

3.1. Flow curves

The flow stress–strain curves of the compressed samples under different conditions are shown in Fig. 2. The general characteristics of the flow curves are similar at all deformation conditions, i.e. the flow stress increases to a peak and then decreases to a steady state, suggesting a typical DRX-accompanied plastic flow process [15]. At any strain rates, the peak stress and peak strain increase along with the decrease of temperature, suggesting that the working hardening effect is more significant at low temperatures. At a given temperature, the peak stress increases along with the increase of strain rate, indicating that the release of work hardening factors like dislocation accumulation is more effective during slower deformation processes. On the other hand, the peak stress is reached at a certain strain that decreases with the increase of temperature or decrease of strain rate. This suggests that DRX proceeds more rapidly at higher temperatures and more extensively at slower strain rate.

The main difference between these states lies in the flow stress value. At the lower temperatures (473 K), the flow stress of the as-cast alloy is higher, owing to β-phase distributing along grain boundaries increasing intercrystalline strengthening. At the high temperature, β-phase becomes soft resulting in plastic deformation easily [16]. Compared to the as-cast alloy, the dislocation density of as-homogenized state is higher owing to solution phase in the interior of grains. The dynamic recrystallization is incomplete at high strain rate and high temperature, so the stress value of as-homogenized alloy is higher than the as-cast alloy. The difference of the stress value is little at low strain rate and high temperature because of the complete dynamic recrystallization, as shown in Fig. 3.

3.2. Processing map

Sivakesavam and Prasad [3] concluded that processing maps made at different strains were essentially similar, and only did the processing map for designed alloy give at one strain in many investigations. The processing maps of the AZ91 alloy deformed at the strain of 0.8 can be obtained by means of overlapping a power dissipation map and an instability map in Fig. 4, in which the shaded domain represents the instable region. The darker colour indicates the greater instability. From processing maps, it can be seen that there are some similarities among different states:

(1) A minimum efficiency of power dissipation can be obtained at low temperature and high strain rate, while a maximum efficiency about 35% of power dissipation can be gained at high temperature and low strain rate. Owing to a few operating slip systems for magnesium alloy at RT, twining is the dominating deformation mode for it in the process of hot working at low temperatures and high strain rates. While other slip systems will be operated with increase of deformation temperature and decrease of strain rate. DRX is also prone to occur in the deformation processing of hot working with increase of deformation temperature and decrease of strain rate. The microstructure

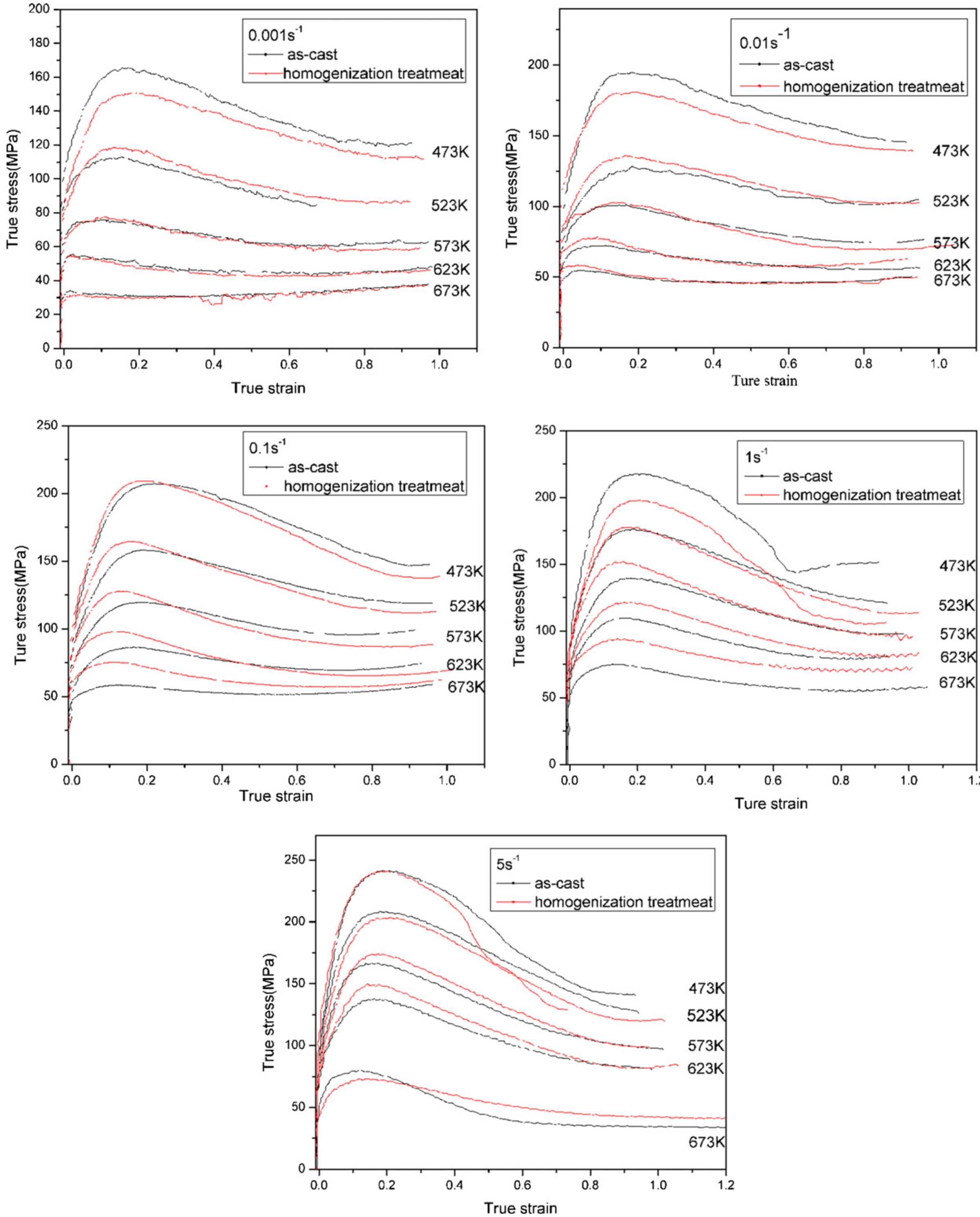

Fig. 2. Flow stress–strain curves of the compressed samples under different compression conditions.

transition of the as-cast alloy hot-deformed at different temperatures with the strain rate of $0.001\,s^{-1}$ is shown in Fig. 5. Obviously, the fraction of DRX increased while the twining decreased with increase of the deformed temperatures. The law of microstructure transition also applies to the as-homogenized state deformation.

(2) The most unstable zone can be obtained as the deformation temperature is low and strain rate is high, and ξ value gradually changes from negative value to positive value with increasing deformation temperature and decreasing strain rate. Because the alloy is deformed at the low temperatures and the high strain rates, in which the value of ξ are negative. According to Prasad, this phenomenon of flow instability is due to the dynamic strain aging and the initiation and growth of micro-cracks [17,18].

The processing maps gained at different states show obviously difference, that is to say, the microstructure transition of the two

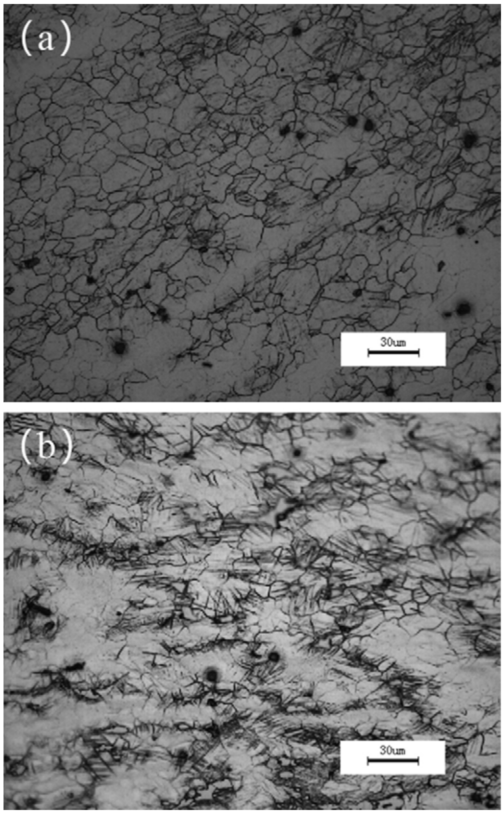

Fig. 3. Typical microstructures of the samples deformed at 0.001 s^{-1} and at the temperatures 673 K: (a) as-cast AZ91 and (b) as-homogenized AZ91.

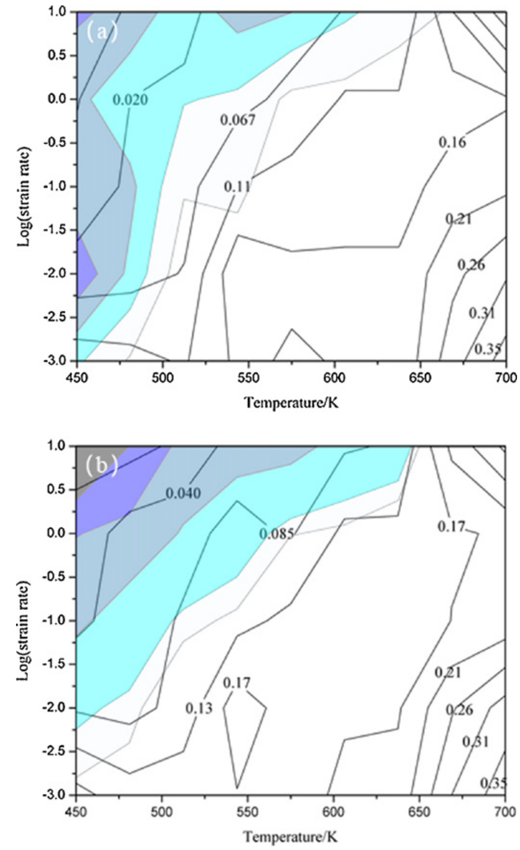

Fig. 4. Processing maps of the alloy at strains of 0.8: (a) as-cast and (b) as-homogenized.

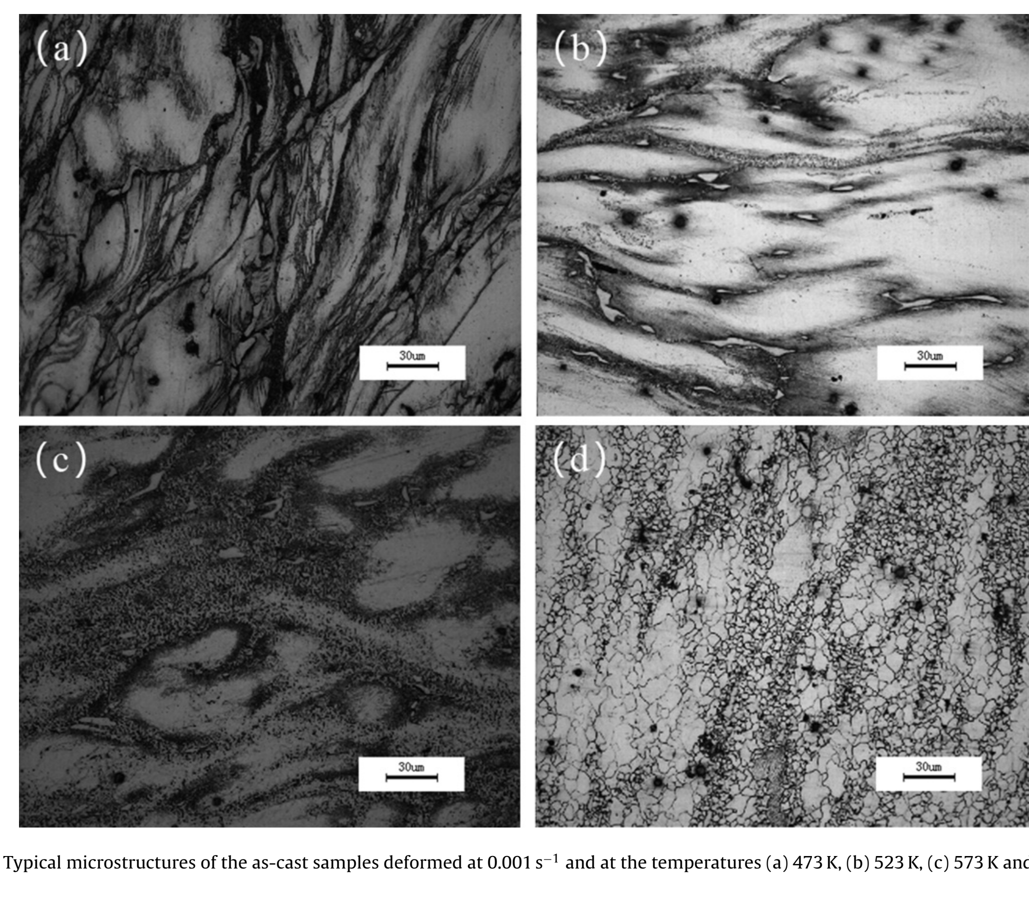

Fig. 5. Typical microstructures of the as-cast samples deformed at 0.001 s^{-1} and at the temperatures (a) 473 K, (b) 523 K, (c) 573 K and (d) 623 K.

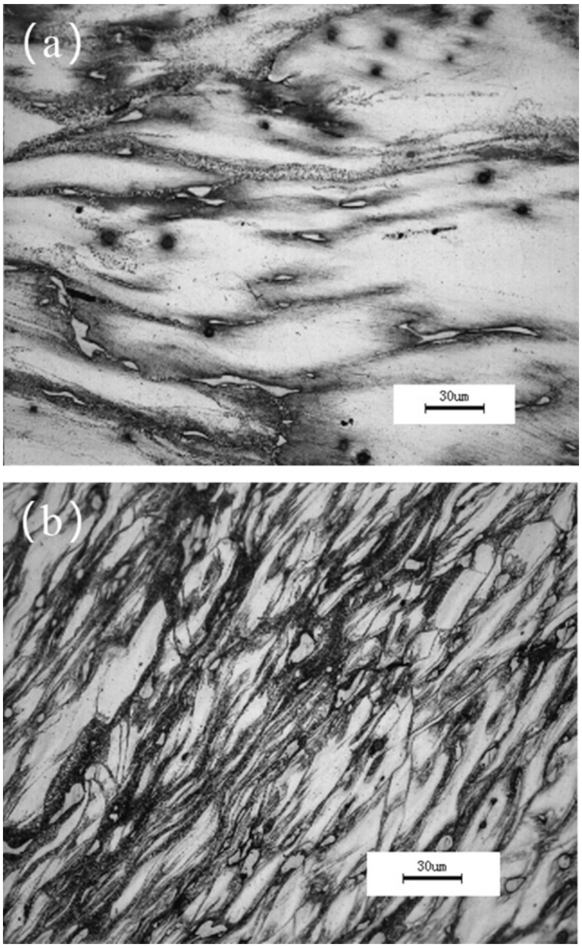

Fig. 6. Typical microstructures of the samples deformed at 0.001 s^{-1} and at the temperatures 523 K: (a) as-cast AZ91 and (b) as-homogenized AZ91.

states deformed with the same conditions is different. These differences are as follow:

(1) When the temperature is below 650 K, the efficiency of power dissipation η of as-homogenized state is greater than the as-cast state under the same deformation conditions. The microstructure of the two states at deformation condition for 523 K/0.001 s^{-1} is given in Fig. 6. Obviously, the fraction of DRX and twining of as-homogenized alloy is greater than the as-cast state, which leads to the large η value. It cannot find the twining when the temperature is above 573 K, but the fraction of DRX of as-homogenized alloy is still greater than the as-cast state, as shown in Fig. 7.

(2) Compared with the as-cast AZ91, the as-homogenized state still owes the characteristics of stable flow at 473 K/0.001 s^{-1}. It is because that AZ91 cast ingot usually contains large amounts of $Mg_{17}Al_{12}$ divorced eutectics distributing along the grain boundary (Fig. 1(a)), which suffers sever cracking and facilities cavity formation due to its incoherency with Mg matrix, which results in crack generation [13]. After homogenization, the AZ91 alloy has a microstructure of few small $Mg_{17}Al_{12}$ (β-phase) particles on grain boundaries (Fig. 1(b)), so it effectively guarantee the stability of the metal flow. The microstructure of the two states after deformation at 473 K/0.001 s^{-1} is given in Fig. 8. Comparing with the as-homogenized state, the larger elongated β-phase along grain boundaries is found in the as-cast AZ91 alloy.

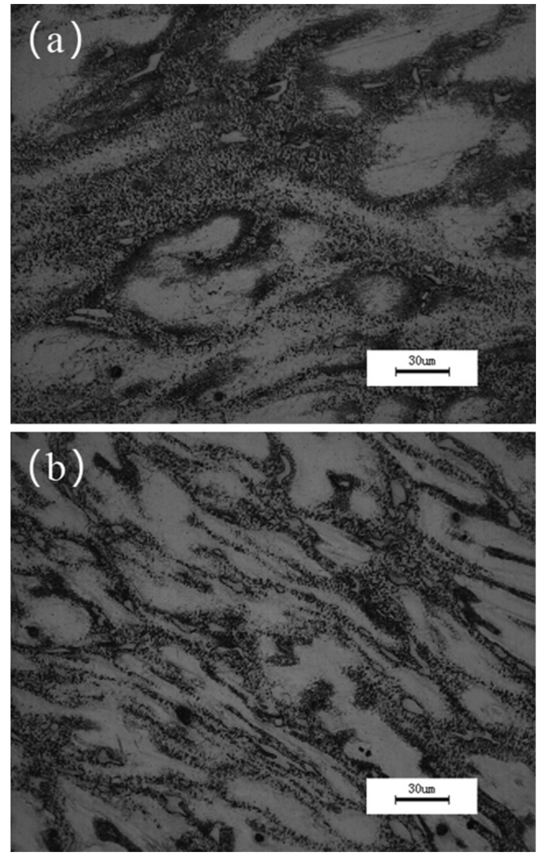

Fig. 7. Typical microstructures of the samples deformed at 0.001 s^{-1} and at the temperatures 573 K: (a) as-cast AZ91and (b) as-homogenized AZ91.

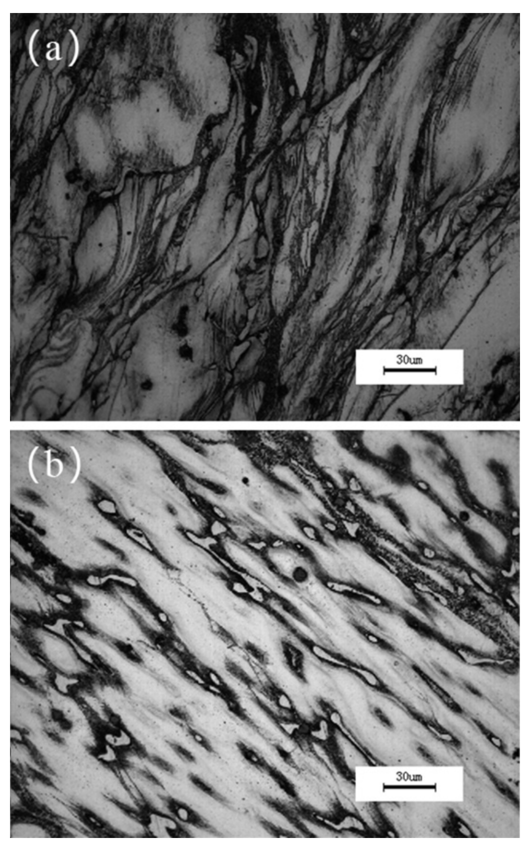

Fig. 8. Typical microstructures of the samples deformed at 0.001 s^{-1} and at the temperatures 473 K: (a) as-cast AZ91 and (b) as-homogenized AZ91.

4. Conclusions

(1) The general characteristics of the flow curves of the two states are similar at all deformation conditions. The main difference is that the flow stress of the as-cast alloy is higher at the lower temperatures (473 K) because of the strengthening β-phase distributing along grain boundaries.

(2) For the two states, the efficiency of power dissipation and the instability parameter all increase along with the increase of temperature and the decrease of strain rate. But the efficiency of power dissipation of as-homogenized state is greater than the as-cast state under the same deformation conditions because of a larger proportion of twining and/or DRX below the temperature of 650 K, and the as-homogenized state still owes the characteristics of stable flow at 473 K/0.001 s^{-1}.

(3) By the processing maps and metallographic observations, both the as-cast AZ91 alloy and the homogenized AZ91 alloy can gain the great η value and stable flow regions with large number of small DRX grains at the temperature range from 623 K to 673 K and the strain rate range from 0.001 s^{-1} to 0.03 s^{-1}.

References

[1] Y.V.R.K. Prasad, K.P. Rao, Mater. Sci. Eng. A 487 (2007) 316–327.
[2] M.R. Barnett, A.G. Beer, D. Atwell, A. Oudin, Scr. Mater. 51 (2004) 19–24.
[3] O. Sivakesavam, Y.V.R.K. Prasad, Mater. Sci. Eng. A 362 (2003) 118–124.
[4] Y.V.R.K. Prasad, K.P. Rao, N. Hort, K.U. Kainer, Mater. Lett. 62 (2008) 4207–4209.
[5] A. Mwembela, E.B. Konopleva, H.J. McQueen, Scr. Mater. 37 (1997) 1789–1795.
[6] Y.V.R.K. Prasad, T. Seshacharyulu, Mater. Sci. Eng. A 243 (1998) 82–88.
[7] Y.V.R.K. Prasad, K.P. Rao, Mater. Sci. Eng. A 391 (2005) 141–150.
[8] J.R. Morris, J. Scharff, K.M. Ho, D.E. Tumer, Philos. Mag. A 76 (1997) 1065–1077.
[9] S.V.S. Narayana Murty, Mater. Sci. Eng. A 254 (1998) 76–82.
[10] H.Z. Li, H.J. Wang, Z. Li, Mater. Sci. Eng. A 528 (2010) 154–160.
[11] Y.V.R.K. Prasad, Indian J. Technol. 28 (1990) 435–451.
[12] Y.V.R.K. Prasad, H.L. Gegel, S.M. Doraivelu, Metall. Trans. A15 (1984) 1883–1892.
[13] A. Srinivasan, J. Swaminathan, M.K. Gunjan, Mater. Sci. Eng. A 527 (2010) 1395–1403.
[14] M.D. Nave, A.K. Dahle, D.H. St John, in: I. Howard, N. Kaplan, John, B. Hryn, Byron, Clow (Eds.), Proceedings of the Symposium on Magnesium Technology 2000, TMS, Nashville, 2000, pp. 233–242.
[15] T. Sakai, J.J. Jonas, Acta Metall. 32 (1984) 189–209.
[16] X.F. Huang, Q.D. Wang, C. Lu, Chin. J. Mater. Res. 18 (2004) 630–634.
[17] Y.V.R.K. Prasad, J. Mater. Process 12 (2003) 638–645.
[18] S. Ramanathan, R. Karthikeyan, G. Ganesan, Mater. Sci. Eng. A 441 (2006) 321–325.